EUROPEAN ORGANIZATION FOR NUCLEAR RESEARCH

CERN–PPE/93–135
30 July 1993

A HIGH-RESOLUTION DETECTOR BASED ON LIQUID-CORE SCINTILLATING FIBRES WITH READOUT VIA AN ELECTRON-BOMBARDED CHARGE-COUPLED DEVICE

C. Cianfarani[1], A. Duane[2], J.-P. Fabre[3], A. Frenkel[1], S.V. Golovkin[4], A.M. Gorin[4], K. Harrison[1], E.N. Kozarenko[5], A.E. Kushnirenko[4], E.A. Ladygin[5], G. Martellotti[1], A.M. Medvedkov[4], P.A. Nass[6], V.P. Obudovski[5], G. Penso[1], Yu.P. Petukhov[5], W.P. Siegmund[7], V.E. Tyukov[5] and V.G. Vasilchenko[4]

Abstract

This paper is a presentation of results from tests in a 5 GeV/c hadron beam of detectors based on liquid-core scintillating fibres, each fibre consisting of a glass capillary filled with organic liquid scintillator. Fibre readout was performed via an Electron-Bombarded Charge-Coupled Device (EBCCD) image tube, a novel instrument that combines the functions of a high-gain, gated image intensifier and a Charge-Coupled Device. Using 1-methylnaphthalene doped with 3 g/ℓ of R45 as liquid scintillator, the attenuation lengths obtained for light propagation over distances greater than 16 cm were 1.5 m in fibres of 20 μm core and 1.0 m in fibres of 16 μm core. For particles that crossed the fibres of 20 μm core at distances of ~1.8 cm and ~95 cm from the fibres' readout ends, the recorded hit densities were 5.3 mm^{-1} and 2.5 mm^{-1} respectively. Using 1-methylnaphthalene doped with 3.6 g/ℓ of R39 as liquid scintillator and fibres of 75 μm core, the hit density obtained for particles that crossed the fibres at a distance of ~1.8 cm from their readout ends was 8.5 mm^{-1}. With a specially designed bundle of tapered fibres, having core diameters that smoothly increase from 16 μm to 75 μm, a spatial precision of 6 μm was measured.

(Submitted to Nuclear Instruments and Methods in Physics Research)

[1] Università di Roma 'La Sapienza' and INFN, Rome, Italy.
[2] Imperial College, London, UK
[3] CERN, Geneva, Switzerland.
[4] IHEP, Protvino, Moscow region, Russia.
[5] JINR, Dubna, Moscow region, Russia.
[6] Schott Glaswerke, Mainz, Germany
[7] Schott Fiber Optics Inc., Southbridge, MA, USA.

1 INTRODUCTION

In the past few years much progress has been made in developing high-resolution detectors based on coherent bundles of liquid-core scintillating fibres [1–8]. The fibres used have diameters of 15–200 μm and are formed from thin-walled, narrow-bore, glass filled with organic liquid scintillator: capillary walls and liquid scintillator constitute a fibre's cladding and core respectively. Track images produced at the end face of a bundle of scintillating fibres traversed by ionizing particles may be recorded via an optoelectronic system.

Scintillating-fibre devices show promise for high-energy physics applications [1, 2, 9–14] — both in current experiments and at proposed future high-luminosity facilities such as the Large Hadron Collider (LHC) and the Superconducting Super Collider (SSC) — and for medical imaging [15]. After overcoming the technical complications involved in filling capillaries with liquid, liquid-core fibres offer performance characteristics that surpass those of the best glass and plastic scintillating fibres currently available. With an appropriate choice of liquid scintillator and capillary glass it is possible to obtain high light yield (>10 photons per keV), fast response (~6 ns), a reasonable efficiency for the trapping of light in fibres (~7% in each direction), and exceptional radiation resistance (doses of >600 kGy tolerated [16]). The excellent quality of the core-cladding interface in liquid-core fibres is conducive to long light-attenuation lengths: for capillaries with diameters of 20 μm and 150 μm, attenuation lengths of 1.5 m and 2.25 m respectively have been measured [16]. Insertion of black glass in the interstices between capillaries in a bundle of liquid-core fibres effectively eliminates crosstalk, ensuring that background noise is low [6].

In a typical readout system, a series of image intensifiers amplifies the light emergent from the scintillating fibres so that it may be registered by a Charge-Coupled Device (CCD). The major part of the light amplification is usually performed by an image intensifier that contains a microchannel plate. Image intensifiers of this type can be gated and consequently allow for triggered readout. Drawbacks of image intensifers with microchannel plates are that they suffer from poor spatial resolution and large fluctuations in gain.

Event buffering in fibre readout, essential for high-rate applications, is being made possible through the development of optoelectronic image-delay tubes [17–19].

In this paper results are presented from tests in a 5 GeV/c hadron beam at the CERN Proton Synchrotron of detectors based on liquid-core fibres with the first use made of a readout system that includes an Electron-Bombarded Charge-Coupled Device (EBCCD) image tube, a novel instrument that combines the functions of a large-gain, gated image intensifier and a CCD. Tests have been carried out for bundles of fibres having core diameters of 16 μm and 20 μm, and for a specially designed bundle of tapered fibres having core diameters that increase smoothly from 16 μm to 75 μm. With the tapered fibres it was possible to have an initial magnification of track images, and so improve resolution while avoiding the light losses due to coupling inefficiencies suffered by systems where magnifying elements and fibres are separate [7]. Use has been made of two newly synthesized liquid scintillators: one containing the proprietary solute R39, the other the proprietary solute R45.

2 LIQUID-CORE SCINTILLATING FIBRES

Three bundles of liquid-core scintillating fibres have been tested. All bundles were of hexagonal cross-section. The capillaries present in each bundle were fabricated[1] from borosilicate glass, refractive index 1.49, and were circular in cross-section. The inner and outer dimensions of the capillaries were respectively 20 μm and 28 μm in one bundle; 16 μm and 20 μm in a second bundle. The former bundle had a length of 104 cm and a cross-sectional area of 27.4 mm^2; the latter had a length of 86 cm and its cross-sectional area was 10.4 mm^2. In the third bundle the capillaries were gently tapered and their inner and outer diameters were respectively 16 μm and 20 μm at one end, 75 μm and 90 μm at the other end. This bundle had a length of 40 cm, and its cross-sectional area varied between 10.4 mm^2 where the capillaries were narrowest and 259.8 mm^2 where the capillaries were widest.

Fabrication of a bundle of liquid-core fibres commences with the production of glass capillaries that have circular cross-sections measuring a few millimetres in diameter. The capillaries are stacked in groups of about a hundred to form mini-bundles. Mini-bundles are drawn, packed together, and then further drawn to give the final array of narrow-diameter capillaries. In order to keep the ratio of pore diameter to wall thickness as large as possible for the capillaries, it is necessary for relatively high stresses to be used in the last drawing stage. In this way the surface tension that tends to reduce the area of the capillary pores is overcome. However, the high drawing stresses cause the outermost mini-bundles in a capillary array to separate from neighbouring mini-bundles. Gaps then develop between mini-bundles; the capillary arrays become more susceptible to breakage around their edges and have a degraded packing fraction (defined for a scintillating-fibre detector as the ratio between the detector's active volume and its total volume). In an attempt to improve the situation, a modified technique for producing capillary arrays has been tried. In this case each capillary is formed from two layers of borosilicate glass, rather than from the usual single layer. The glass of the outer layer has a lower melting point and is more adhesive than the glass of the inner layer. The increased adhesion of the glass on the capillaries' outer surfaces strengthens the bonding between mini-bundles and reduces the likelihood of their separating.

Single layers of glass were used in producing the capillaries of 20 μm bore; double layers of glass were used in forming the capillaries of 16 μm bore and the tapered capillaries. The packing fraction was increased from ~50% for the bundle containing the capillaries of 20 μm bore to ~60% for the other two bundles. In all of the bundles, black glass was introduced into a fraction of the interstices between capillaries so as to suppress any crosstalk.

Two newly synthesized liquid scintillators[2] were tested. The tapered capillaries were filled with 1-methylnaphthalene (1MN, refractive index 1.62) doped with 3.6 g/ℓ of R39; the other capillaries were filled with 1MN doped with 3 g/ℓ of R45. The scintillator that had R39 as solute was characterized by a higher light yield but a shorter light-attenuation length than the scintillator that contained R45. Both scintillators emitted in the green region, with peak emission at around 500 nm. The emission spectra were well matched to the ranges of greatest sensitivity of available image-intensifier photocathodes. Scintillators that emit in the green region are also of interest because they can have enhanced radiation resistance. The solute concentrations used ensured that light emission was local to points

[1] Schott Fiber Optics Inc., Southbridge, MA, USA.

[2] Geosphaera, Moscow, Russia.

of energy deposition, a condition that is necessary when high resolution is sought.

Taking into account meridional and skew rays, the efficiency for trapping light in the fibres tested was ~7.5% in each direction, this being determined by the shape of the fibre cross-sections and by the ratio of the refractive index of the core to that of the cladding.

3 OPTOELECTRONIC READOUT SYSTEM

Fibre readout was performed using an optoelectronic system (Fig. 1) which, in order of increasing distance from the fibre ends, was composed of an electrostatically focused image intensifier[3] ($I I_1$), a fibre-optic taper[4], two further electrostatically focused image intensifiers[3] ($I I_2$, $I I_3$), and an EBCCD image tube[3]. All of the image intensifiers had fibre-optic input and output windows and multialkali photocathodes.

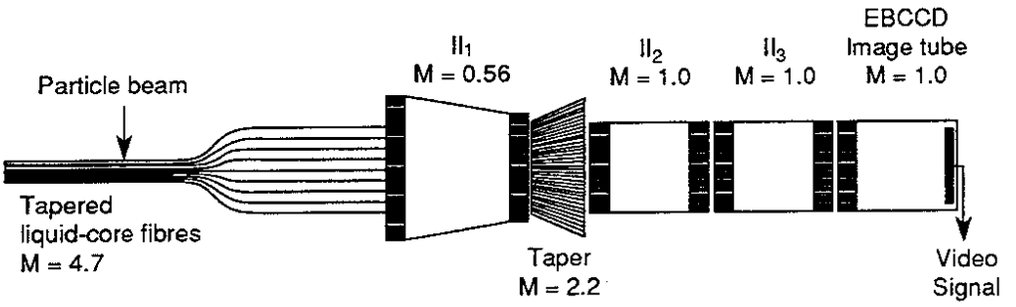

Figure 1: Bundle of tapered fibres and optoelectronic readout system. The magnification, M, of each component is noted.

The image intensifier $I I_1$, which had an entrance window of 40 mm diameter and an exit window of 25 mm diameter, demagnified images generated at the end faces of the fibre bundles by a factor of 1.8. The demagnification that it provided was not useful, but in other respects $I I_1$ had excellent specifications. The phosphor had a decay-time constant of 50 ns and, including transmission losses at the input window, the quantum efficiency of the photocathode was 20% for light of 500 nm wavelength .

The fibre-optic taper placed after $I I_1$ magnified images by a factor of 2.2 and so improved resolution. The taper, which had a transparency of ~50% averaged over the emission spectrum of the phosphor of $I I_1$, was composed of fibres that had square cross-sections, these having sides of ~4.0 μm at the input and ~8.6 μm at the output. The diameters of the taper's circular entrance and exit faces were 19 mm and 41 mm respectively.

The image intensifiers $I I_2$ and $I I_3$ were of the same type. They had entrance and exit windows of 25 mm diameter and gave magnification 1. The decay-time constant of the image-intensifier phosphors was 700 ns. The main function of $I I_2$ and $I I_3$ was to delay the optical signal from the fibres for the time necessary (~400 ns) to trigger reading of the EBCCD image tube.

The EBCCD image tube (Fig. 2) is essentially an electrostatically focused image intensifier that, in place of a phosphor, has a specially treated CCD. For the tests described, use was made of a buried-channel CCD that had an image zone of 290 × 532 pixels, each pixel having dimensions of 23 × 17 μm^2. The CCD was thinned to a thickness of 12 μm and was mounted in the EBCCD image tube so that its reverse surface was struck by

[3] Geosphaera, Moscow, Russia.

[4] Schott Fiber Optics Inc., Southbridge, MA, USA.

electrons released at the photocathode. All of the CCD's reverse face was sensitive to photoelectrons — in contrast to the situation with a phosphor, where there may be dead regions between phosphor grains. The EBCCD image tube gave unit magnification and for the operating voltage of 10 kV had a gain of 2000. The EBCCD image tube could be gated on or off by applying appropriate voltage pulses to one of the focusing electrodes. During tests the EBCCD image tube was gated off unless trigger conditions were satisfied, when it was gated on for 3 μs. The CCD readout electronics have been fully described elsewhere [20].

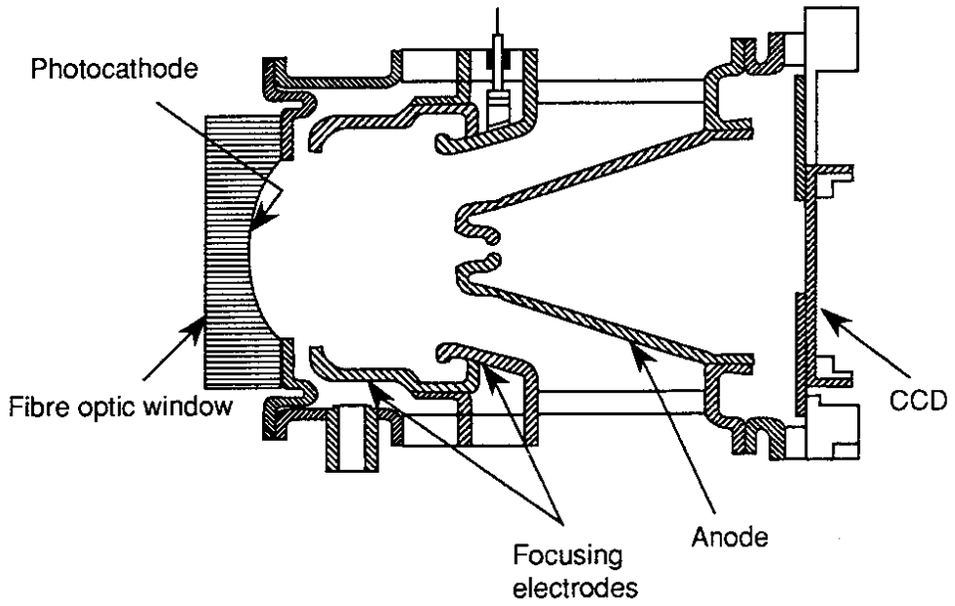

Figure 2: EBCCD image tube.

An EBCCD image tube is a substitute in a scintillating fibre readout system for an image intensifier that contains a microchannel plate and a CCD, the functions of which it combines. Avoiding utilization of an image intensifier containing a microchannel plate is advantageous. Compared to such an image intensifier an EBCCD image tube offers higher spatial resolution and lower gain fluctuations, and there is none of the noise that arises from electrons being backscattered at the phosphor screen of an image intensifier that is proximity focused. The lifetime of an EBCCD image tube is at least equal to that of a device containing a microchannel plate — after 2000 hours of operation in a flux of 10^{-2} lux the dark current is increased by less than a factor of 2 and remains below 1% of the saturation level. Unlike an image intensifier that contains a microchannel plate, the gain of which is reduced with age, the gain of an EBCCD image tube is constant during the instrument's lifetime.

4 ANALYSIS AND RESULTS

Each of the fibre bundles tested was in turn positioned so as to be perpendicularly crossed by 5 GeV/c hadrons. Images of single particle tracks (Fig. 3) were recorded for hadrons that entered the bundles at different distances d from the fibres' readout ends. The tapered fibres were viewed with their wider ends coupled to the input window of $\mathrm{I\,I_1}$. This meant that the track images of particles that traversed the tapered fibres' narrower ends were magnified by a factor of 4.7 (the ratio of a tapered fibre's core diameter at its

wider end to that at its narrower end) in addition to the overall magnification of $\times 1.2$ introduced by the readout system.

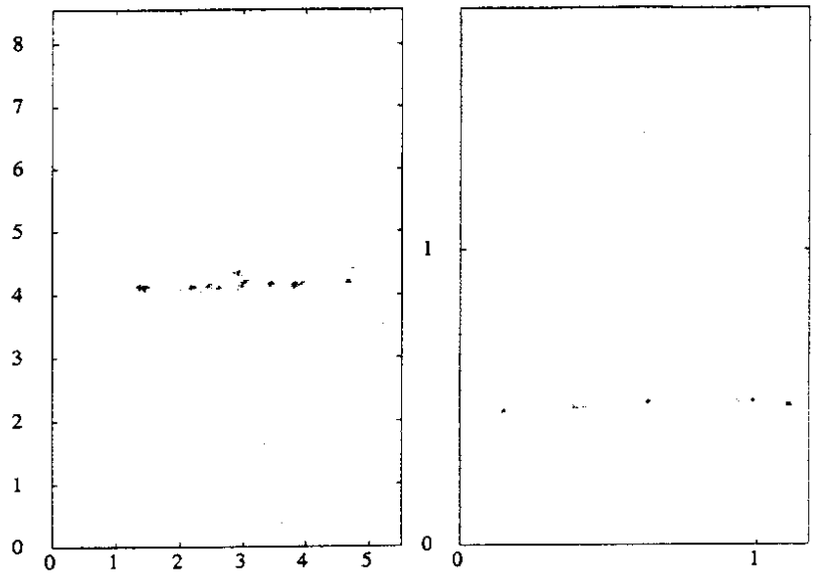

Figure 3: Track images produced by 5 GeV/c hadrons travelling perpendicularly to fibre axes at a distance of ~30 cm from the fibres' readout ends: using capillaries of 20 μm bore filled with R45-doped 1MN and with image magnification $\times 1.2$ at the EBCCD (left); using capillaries of 16 μm bore filled with R39-doped 1MN and with image magnification $\times 5.7$ at the EBCCD (right). Scales are in millimetres in real space and the entire image zone is shown in both cases.

Reconstruction and analysis of the single-particle tracks has been performed using the established procedures [20–22]. A photoelectron detected at the phosphor of $\mathrm{I\,I_1}$ gave rise to a cluster of lit pixels at the EBCCD and will be referred to as a hit. Hits were first individuated in the analysis as local maxima in the pulse height. Clusters were obtained by grouping lit pixels about such local maxima and cluster barycentres were identified with the positions of hits. A cluster that consisted of fewer than three pixels was attributed to low-level, electronic noise and was disregarded. Tracks were given by unweighted, linear fits to hits that were approximately aligned. The analysis allowed determination (Table 1) of root-mean-square (r.m.s.) track residuals, two-track resolutions, hit densities as a function of the distance d, and light-attenuation lengths in the fibres. Measurement errors were of the order of 10–15%, except for the attenuation lengths where uncertainties were larger (25–40%).

Track residuals measure the displacements of hits from fitted tracks. For the fibre bundles tested the distributions of track residuals consisted of approximately Gaussian peaks superimposed on diffuse backgrounds (Fig. 4). In each case the r.m.s. track residual was evaluated as the peak's full-width-at-half-maximum times $1/\sqrt{8\ln 2}$. The two-track resolution quantifies the combined effect of the spread of clusters about fitted tracks and of the cluster sizes. For each fibre bundle considered, a plot was made of the distribution of pulse height transverse to the direction of fitted tracks (Fig. 5) and the two-track resolution was calculated as $1/\sqrt{8\ln 2}$ times the full-width-at-half-maximum of the peak in the distribution.

Table 1: Characteristics of the liquid-core scintillating fibres tested. In all cases the cladding material was borosilicate glass, the light-trapping efficiency in the fibres was ~7.5% in each direction, and the amount of light associated with noise (essentially from production of delta rays) was less than 10% of the total. Hit densities were measured for particles crossing the fibres at various distances d from the fibres' readout ends. Values in the last two columns refer to different sections of the tapered fibres. Uncertainties in the values quoted for hit densities, r.m.s. track residuals, and two-track resolutions are of the order of 10–15%.

Core diameter (μm)	20	16	75	16
Cladding thickness (μm)	4	2	7.5	2
Liquid scintillator : base	1 MN	1 MN	1 MN	1 MN
: solute	3 g/ℓ R45	3 g/ℓ R45	3.6 g/ℓ R39	3.6 g/ℓ R39
Packing fraction	0.46	0.58	0.63	0.58
Fibre magnification at EBCCD	1.2	1.2	1.2	5.7
r.m.s. track residual (μm)	18	14	28	6
Two-track resolution (μm)	39	33	45	11
Hit density (mm^{-1}) : for $d \sim 1.8$ cm	5.3	–	8.5	–
: for $d \sim 17$ cm	4.4	4.2	–	–
: for $d \sim 30$ cm	3.3	3.4	–	5.5
: for $d \sim 95$ cm	2.5	–	–	–
Attenuation length (m) for $d > 16$ cm	1.5 ± 0.4	1.0 ± 0.4	–	–

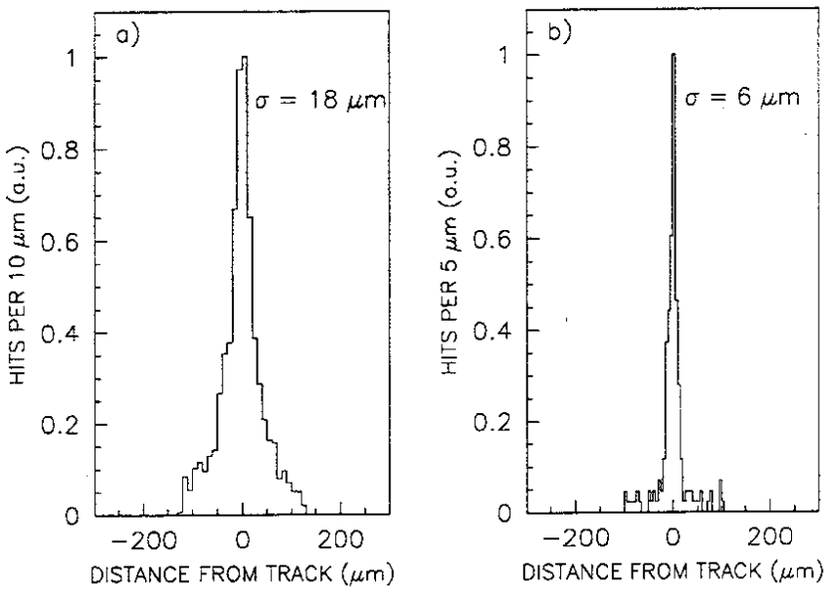

Figure 4: Distributions of track residuals: a) for capillaries of 20 μm bore filled with R45-doped 1MN and with image magnification $\times 1.2$ at the EBCCD; b) for capillaries of 16 μm bore filled with R39-doped 1MN and with image magnification $\times$ 5.7 at the EBCCD. The width, σ, of the peak in each distribution is noted.

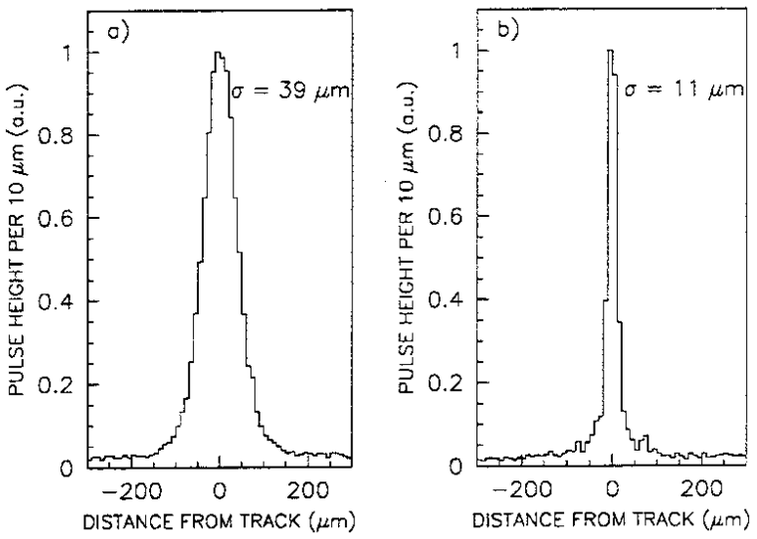

Figure 5: Distributions of pulse height transverse to the direction of fitted tracks: a) for capillaries of 20 μm bore filled with R45-doped 1MN and with image magnification $\times 1.2$ at the EBCCD; b) for capillaries of 16 μm bore filled with R39-doped 1MN and with image magnification $\times$ 5.7 at the EBCCD. The width, σ, of the peak in each distribution is noted.

As measured in real space, the r.m.s. track residuals obtained with the fibres having cores of 20 μm diameter and with those having cores of 16 μm diameter were respectively 18 μm and 14 μm. The r.m.s. track residuals had no significant dependence on the distance d, indicating that fibre coherency remained good along the entire length of each bundle. When particles passed through the narrower ends of the tapered fibres, the large image magnification at the EBCCD improved resolution and the r.m.s. track residual was reduced to 6 μm. This approaches the theoretical limit of 5.33 μm for fibres having circular cross-section and 16 μm core diameter, and represents the highest spatial precision so far recorded for a scintillating-fibre detector. Past experience [6–8] suggests that the detector resolution benefited from the use of the EBCCD image tube, and larger track residuals would have been expected had the EBCCD image tube been replaced by a CCD and an image intensifier containing a microchannel plate. Studies of a grid pattern viewed through the optoelectronic system show that the image intensifiers introduce a small amount of pincushion distortion, but the effect on the r.m.s. track residuals was negligible compared with measurement errors.

Values found for two-track resolutions were greater than the corresponding values for r.m.s. track residuals by factors of between 1.6 and 2.4. This reflects the comparative largeness of the clusters of lit pixels associated with each hit: the r.m.s. cluster size was $\sim$35 μm at the EBCCD.

The number of hits recorded per unit path length traversed by a particle in a scintillating-fibre detector defines a hit density. In determining hit densities, hits displaced from fitted tracks by no more than 3 times the two-track resolution were considered, and the longitudinal distance, ℓ, of each hit from its nearest neighbour was plotted. Disregarding distances that were below a minimum, where there were effects due to coalesced clusters, or above a maximum, where there were poor statistics, the resulting distributions were fitted by exponentials of the form $\sim \exp(-h\ell)$, h being a hit density [21].

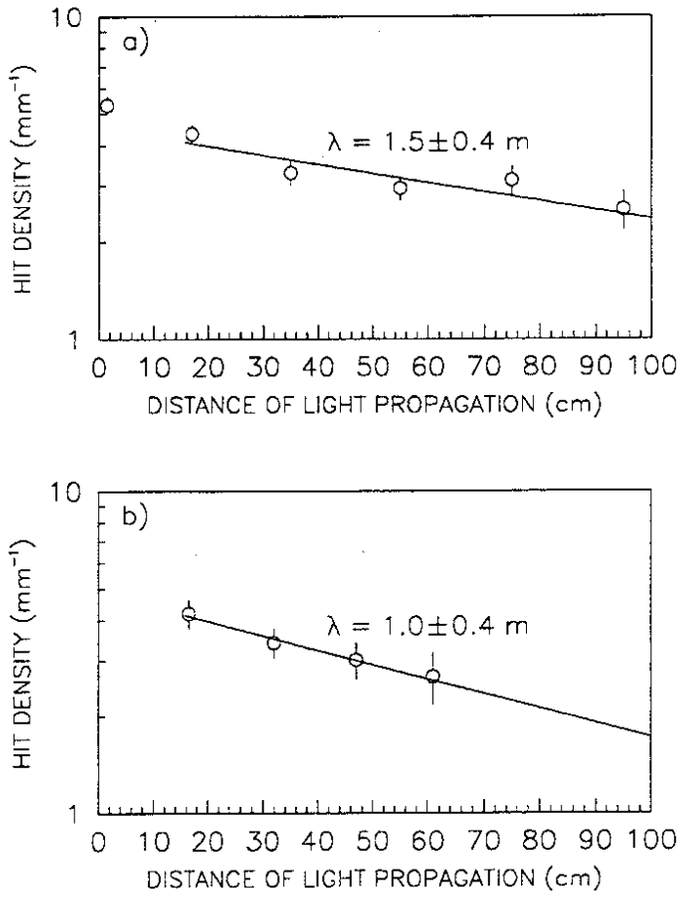

Figure 6: Light-attenuation curves for fibres having liquid cores of 1MN doped with 3 g/ℓ of R45: a) for a core diameter of 20 μm; b) for a core diameter of 16 μm. In each case the attenuation length, λ, has been calculated for light propagation over distances greater than 16 cm.

The attenuation of light within the longer-length fibres was seen in the variation of the hit density with the distance d (Fig. 6). For d >16 cm, the attenuation lengths for the fibres having cores of 20 μm diameter and for those having cores of 16 μm diameter were 1.5 ± 0.4 m and 1.0 ± 0.4 m respectively. Within the errors, the indication is that the worsening of attenuation in the narrower fibres was not excessive. For the fibres having cores of 20 μm diameter, the hit density at $d \sim 95$ cm remained relatively high, at 2.5 mm^{-1}. For $d \sim 1.8$ cm, the hit density was 8.5 mm^{-1} for the tapered fibres, as compared with 5.3 mm^{-1} for the fibres having 20 μm cores. The hit density was greater in the former case because the packing fraction was larger and because the scintillation efficiency of 1MN doped with 3.6 g/ℓ of R39 is higher than that of 1MN doped with 3 g/ℓ of R45.

With all of the fibre bundles tested, the pulse height at the EBCCD due to hits displaced from fitted tracks by more than 3 times the two-track resolution constituted a little under 10% of an image's total pulse height, essentially that expected from the production of delta rays.

5 CONCLUSIONS

An EBCCD image tube has been used for the first time in the triggered readout of particle tracks imaged by a scintillating-fibre detector. The EBCCD image tube functioned well and is believed to have had a beneficial effect on the overall spatial precision.

The great potential for high-resolution tracking applications of detectors based on liquid-core scintillating fibres has been reconfirmed. Using 1MN doped with 3 g/ℓ of R45 as liquid scintillator, the attenuation lengths for light propagation over distances greater than 16 cm were 1.5±0.4 m in fibres having 20 μm core diameter and 1.0±0.4 m in fibres of 16 μm core diameter. For particles that crossed the fibres of 20 μm core at distances of ~1.8 cm and ~95 cm from the fibres' readout ends the calculated hit densities were 5.3 mm^{-1} and 2.5 mm^{-1} respectively. Using 1MN doped with 3.6 g/ℓ of R39 as liquid scintillator and fibres of 75 μm core, the hit density obtained for particles that crossed the fibres at a distance of ~1.8 cm from their readout ends was 8.5 mm^{-1}. This is equivalent to 1 hit per 5×10^{-4} radiation lengths and compares favourably with that achieved using gas chambers and other types of tracking detectors. With a specially designed bundle of tapered fibres, the narrower ends of which had 16 μm cores and a total magnification factor of 5.7 at the EBCCD, an r.m.s. track residual of 6 μm was measured. Delta-ray production in the fibre bundles tested was estimated to account for a little under 10% of the light on recorded images. Contributions from crosstalk and electronic noise were negligible.

Work in progress aims to further improve hit densities, by continuing development of new liquid scintillators, by increasing detector packing fractions — in principle 70–80% may be attained — and by decreasing the refractive index of the glass used in capillary fabrication, so as to have a better efficiency for light trapping. Another objective is to utilize capillaries of narrower bore (~6 μm), to permit additional enhancement of the resolution. A trial experiment is planned in which a detector based on liquid-core scintillating fibres will be used in the identification of charmed particles produced in interactions of high-energy neutrinos. This will permit evaluation of the detector's effectiveness for the study of processes in which there is physics interest.

REFERENCES

[1] Proc. Workshop on Scintillating Fiber Detector Development for the SSC, Batavia, IL, USA, 1988 (FNAL, Batavia, IL, 1989).

[2] Proc. Workshop on Application of Scintillating Fibers in Particle Physics, Blössin, Germany, 1990, Ed. R. Nahnhauer (IHEP, Berlin-Zeuthen, Germany, 1990).

[3] D. Puseljic et al., IEEE Trans. Nucl. Sci. **NS-37** (1990) 139.

[4] S.V. Golovkin et al., Nucl. Instr. and Meth. **A305** (1991) 385.

[5] J. Bähr et al., Nucl. Instr. and Meth. **A306** (1991) 169.

[6] M. Adinolfi et al., Nucl. Instr. and Meth. **A311** (1992) 91.

[7] M. Adinolfi et al., Nucl. Instr. and Meth. **A315** (1992) 177.

[8] N.I. Bozhko et al., Nucl. Instr. and Meth. **A317** (1992) 97.

[9] J. Kirkby, Proc. Workshop for the INFN ELOISATRON project: Vertex detectors, Erice, Italy, 1986 (Plenum, New York, 1988), p.225.

[10] R. Ruchti et al., IEEE Trans. Nucl. Sci. **NS-35** (1988) 441.

[11] J. Alitti et al., Nucl. Instr. and Meth. **A279** (1989) 364.

[12] C. Angelini et al., Nucl. Instr. and Meth. **A289** (1990) 342.

[13] N. Armenise et al., Proposal CERN-SPSC/90-42 SPSC P254 (1990).

[14] C. D'Ambrosio et al., Nucl. Instr. and Meth. **A322** (1992) 20.

[15] H. Shao et al., IEEE Trans. Nucl. Sci. **NS-38** (1991) 845.

[16] S.V. Golovkin et al., Proc. Second Workshop on Physics at VLEPP, Protvino, Russia, 1992, Vol. 2, p.117.

[17] J.-P. Fabre et al., Rev. Phys. Appl. **24** (1989) 1019.

[18] T. Gys et al., CERN/DRDC 92-42 LAA/Status Report (1992).

[19] A.G. Berkovski et al., to be submitted to Nucl. Instr. and Meth.

[20] A.G. Denisov et al., Nucl. Instr. and Meth. **A310** (1991) 479.

[21] M.N. Atkinson et al., Nucl. Instr. and Meth. **A263** (1988) 333.

[22] C. Angelini et al., Nucl. Instr. and Meth. **A295** (1990) 299.